

Impurity-induced states in superconducting heterostructures

Dong E. Liu,¹ Enrico Rossi,² and Roman M. Lutchyn¹

¹Station Q, Microsoft Research, Santa Barbara, California 93106-6105, USA

²Department of Physics, College of William & Mary, Williamsburg, Virginia 23187, USA



(Received 29 November 2017; published 26 April 2018)

Heterostructures allow the realization of electronic states that are difficult to obtain in isolated uniform systems. Exemplary is the case of quasi-one-dimensional heterostructures formed by a superconductor and a semiconductor with spin-orbit coupling in which Majorana zero-energy modes can be realized. We study the effect of a single impurity on the energy spectrum of superconducting heterostructures. We find that the coupling between the superconductor and the semiconductor can strongly affect the impurity-induced states and may induce additional subgap bound states that are not present in isolated uniform superconductors. For the case of quasi-one-dimensional superconductor/semiconductor heterostructures we obtain the conditions for which the low-energy impurity-induced bound states appear.

DOI: [10.1103/PhysRevB.97.161408](https://doi.org/10.1103/PhysRevB.97.161408)

Composite heterostructures provide an opportunity to realize states with novel and desirable properties that are different from the individual components. In the past decade, this principle has been implemented successfully to obtain *composite electronic systems* with novel and unique electronic properties. For example, heterostructures comprising a conventional *s*-wave superconductor (SC) and a semiconductor (SM) with strong spin-orbit coupling (SOC) may realize topological superconducting states supporting Majorana zero modes (MZMs)[1–9] of which preliminary signatures have been observed [10–24].

The presence of impurities is unavoidable in any condensed-matter system. However, in heterostructures their effect can be particularly nontrivial due to the interplay between scattering processes involving different materials. Their effect in general varies significantly depending on the component of the heterostructure in which they are located. This fact makes the understanding of impurity effects in superconducting heterostructures nontrivial and outside the scope of most previous works focusing on impurity effects in single-component homogeneous superconducting systems (for a recent review see Ref. [25]).

In this Rapid Communication we study the states induced by scalar impurities in heterostructures involving a SC and a SM with Rashba SOC. Previous studies mostly focused on the case of impurities located in the SM or at the SM/SC interface [26–43]. Here we consider in detail also the case when impurities are located in the SC. We focus on the case of an isolated impurity problem and obtain analytical results that help to understand some recent numerical simulations [44]. We show that in general the self-energy describing the effect of an isolated impurity consists of two terms that may have opposite signs. We find that the complete or partial cancellation of these two terms is responsible for the presence of low-energy impurity-induced states that are not present in homogeneous SC systems [25]. We find that this cancellation may lead to impurity-induced subgap states even in the limit of a vanishing magnetic field. This finding does

not contradict Anderson’s result [45] given that in our system the superconducting order parameter is not uniform. For the specific case of one-dimensional (1D) heterostructures we study how the spectrum of the impurity-induced states changes as a function of an external magnetic field. As shown in Refs. [46–49], a magnetic field may induce a quantum phase transition from a conventional (trivial) superconducting phase to a topological superconducting phase characterized by the presence of MZMs. We identify the regions in parameter space where very low-energy impurity-induced states might affect the observation and manipulation of MZMs.

The Hamiltonian H for the heterostructure can be written as $H = H_N + H_{SC} + H_T$, where H_N is the Hamiltonian for the normal, i.e., nonsuperconducting, component (either a SM or a metal), H_{SC} is the Hamiltonian for the SC, and H_T is the term describing tunneling processes between the SC and the normal component. Specifically, H_N and H_{SC} are defined as (henceforth $\hbar = 1$)

$$H_N = \frac{1}{2} \sum_{\mathbf{k}} \psi_{N,\mathbf{k}}^\dagger [\epsilon_{N,\mathbf{k}} \sigma_0 \tau_z + \alpha \mathbf{k} \cdot \boldsymbol{\sigma} \tau_z + V_x \sigma_x \tau_z] \psi_{N,\mathbf{k}}, \quad (1)$$

$$H_{SC} = \frac{1}{2} \sum_{\mathbf{k}} \psi_{SC,\mathbf{k}}^\dagger [\epsilon_{SC,\mathbf{k}} \tau_z \sigma_0 - \Delta_0 \tau_y \sigma_y] \psi_{SC,\mathbf{k}}. \quad (2)$$

where $\psi_{\mathbf{k},i}^\dagger = (c_{i,\mathbf{k}\uparrow}^\dagger, c_{i,\mathbf{k}\downarrow}^\dagger, c_{i,-\mathbf{k}\uparrow}, c_{i,-\mathbf{k}\downarrow})$ is the spinor with $i = N$ or $i = SC$, $c_{i,\mathbf{k}\sigma}^\dagger$ ($c_{i,\mathbf{k}\sigma}$) is the creation (annihilation) operator for an electron with momentum \mathbf{k} and spin σ in the i th part of the heterostructure, $\epsilon_{i,\mathbf{k}} = (\mathbf{k}^2/2m_i - \mu_i)$ with m_i , μ_i are the electron’s effective mass and chemical potential, respectively, in the i th component, σ_j (τ_j) are the Pauli matrices in spin (Nambu) space, α is the strength of the Rashba SOC with $\mathbf{k} = (0, k_z, -k_y)$, Δ_0 is the amplitude of the superconducting gap, and V_x is the Zeeman splitting due to the external magnetic field along the x direction.

The tunneling Hamiltonian can be written as

$$H_T = \frac{1}{2} \sum_{\mathbf{k}} \psi_{\text{SC},\mathbf{k}}^\dagger \hat{h}_T(\mathbf{q}) \psi_{\text{N},\mathbf{k}+\mathbf{q}} + \text{H.c.}, \quad (3)$$

where $\hat{h}_T(\mathbf{q})$ is the tunneling matrix. In our case, assuming that the tunneling processes conserve the spin and the momentum parallel to the SC-N interface (\mathbf{k}_\parallel) we have $\hat{h}_T(\mathbf{q}) = t\sigma_0\tau_z\delta(\mathbf{q}_\parallel)$ with t being the tunneling amplitude. To quantify the effect of the tunneling term it is helpful to introduce the parameter $\Gamma_i \equiv t^2\rho_{F,\text{SC}}$, where $\rho_{F,\text{SC}}$ is the density of states (DOS) of the SC at the Fermi energy $E_{F,\text{SC}}$.

In the presence of impurities, the Hamiltonian for the system is modified by an additional term H_{imp} , describing the scattering of electrons off the impurities. For a single isolated impurity located in the i th ($i = \text{N,SC}$) component of the heterostructure,

$$H_{\text{imp}} = \sum_{\mathbf{r}} \delta(\mathbf{r}) \psi_{i,\mathbf{r}}^\dagger \hat{h}_{\text{imp}} \psi_{i,\mathbf{r}} = \sum_{\mathbf{k},\mathbf{k}'} \psi_{i,\mathbf{k}}^\dagger \hat{h}_{\text{imp}} \psi_{i,\mathbf{k}'}. \quad (4)$$

Here $\psi_{i,\mathbf{r}}^\dagger$ ($\psi_{i,\mathbf{r}}$) is the creation (annihilation) operator for an electron at position \mathbf{r} in the i th component of the heterostructure, and \hat{h}_{imp} is the matrix describing the structure of the impurity in spinor space. For a scalar impurity, using the convention specified above for spinors, we have $\hat{h}_{\text{imp}} = u_{\text{imp}}\sigma_0\tau_z$ where u_{imp} is the strength of the impurity potential.

The spectrum of the impurity-induced states can be obtained by locating the poles of the T matrix (see the Supplemental Material [50] Sec. I). Using the diagrammatic approach, one can express the T matrix in terms of the Green's function for the isolated components of the heterostructure $G_i^{(0)}(\mathbf{k},\omega) = (\omega + i\eta - H_i)^{-1}$ with $i = \text{N,SC}$ and $\eta \rightarrow 0$. If the impurity is located in the i th component of the heterostructure, the matrix T_i is given by

$$T_i(\omega) = [\mathbb{1} - \hat{h}_{\text{imp}}\Sigma_{i,\text{imp}}(\omega)]^{-1}\hat{h}_{\text{imp}}, \quad (5)$$

where $\Sigma_{i,\text{imp}}(\omega) = \int d\mathbf{k} G_i(\mathbf{k},\omega)$ and $G_i(\mathbf{k},\omega)$ is the Green's function of the i th component of the heterostructure dressed by the self-energy $\Sigma_{i,t}(\mathbf{k}_\parallel,\omega)$ due to the tunneling term,

$$G_i(\mathbf{k},\omega) = \{[G_i^{(0)}(\mathbf{k},\omega)]^{-1} - \Sigma_{i,t}(\mathbf{k},\omega)\}^{-1} \quad (6)$$

$$\Sigma_{i,t}(\mathbf{k},\omega) = \int d\mathbf{q} \hat{h}_T(\mathbf{q}) G_i^{(0)}(\mathbf{k} + \mathbf{q},\omega) \hat{h}_T(-\mathbf{q}). \quad (7)$$

Here $G_i^{(0)}$ is the Green's function of the heterostructure's component coupled via the tunneling term to the i th component. Using Eq. (3), we obtain

$$\Sigma_{i,t}(\mathbf{k}_\parallel,\omega) = t^2 \int d\mathbf{q}_\perp \sigma_0\tau_z G_i^{(0)}(\mathbf{k}_\parallel,\mathbf{q}_\perp,\omega) \sigma_0\tau_z. \quad (8)$$

To understand how the presence of the tunneling term affects the spectrum of the impurity-induced states it is useful to express T_i in the following equivalent form:

$$T_i = \{\mathbb{1} - \hat{h}_{\text{imp}}[\Sigma_{i,\text{imp}}^{(0)}(\omega) + \Sigma_{i,\text{imp}}^{(1)}(\omega)]\}^{-1}\hat{h}_{\text{imp}}, \quad (9)$$

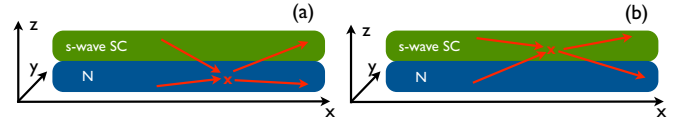


FIG. 1. Sketch of the 1D N/SC heterostructure with an isolated impurity, shown by the red “X” in the semiconductor (N) in (a) and in the SC in (b). The red arrows represent impurity-induced scattering processes.

where

$$\Sigma_{i,\text{imp}}^{(0)}(\omega) = \int d\mathbf{k} G_i^{(0)}(\mathbf{k},\omega), \quad (10)$$

$$\Sigma_{i,\text{imp}}^{(1)}(\omega) = \int d\mathbf{k} G_i^{(0)}(\mathbf{k},\omega) \Sigma_{i,t}(\mathbf{k},\omega) G_i(\mathbf{k},\omega). \quad (11)$$

As follows from above, there are two contributions that determine the pole structure of T_i : $\Sigma_{i,\text{imp}}^{(0)}$ is the term that appears if the component i were isolated, and $\Sigma_{i,\text{imp}}^{(1)}$ is the term due to tunneling processes between the i th and the \bar{i} th components of the heterostructure. If tunneling is not a weak perturbation, the interplay between these two terms may lead to unusual properties for the spectrum of the impurity-induced states in the heterostructure.

For the case when the impurity is located in the normal component (in the remainder we assume it to be a semiconductor) the effect of the tunneling term is to induce a SC gap in it (Δ_{ind}) and it is straightforward from Eq. (5) to obtain $T_{\text{N}}(\omega) = [\tau_z\sigma_0 - u_{\text{imp}}\hat{\Sigma}_{\text{N,imp}}(\omega)]^{-1}u_{\text{imp}}$. When no SOC is present ($\alpha = 0$), $T_{\text{N}}(\omega)$ does not have poles ω^* below the induced gap (i.e., $|\omega^*| \geq \Delta_{\text{ind}}$). In the presence of SOC the induced superconductivity in the SM will be a mix of spin-singlet and spin-triplet pairing components even though in the SC only s -wave pairing is present [51–53]. To further investigate this case we consider the quasi-1D system shown in Fig. 1 in which $L_x \rightarrow \infty$ and L_y, L_z are small enough so that the spectrum is composed of 1D subbands $\epsilon_{k_x}^{(n)}$ with energy separation larger than Δ_0 . For concreteness, in the remainder we limit ourselves to the case in which only one spinful subband is occupied. When V_x is larger than a critical value V_x^c , the system is expected to be in a topological phase [48,49]. For parameter values relevant for current experiments (see the Supplemental Material [50] Sec. II) for $V_x < V_x^c$ the impurity-induced states have energies ω^* , very close to the induced-gap edge. When the chemical potential is much larger than the SC bulk gap (see the Supplemental Material [50] Sec. III), in the trivial regime, $|\omega^*|$ can be smaller than Δ_{ind} , albeit it does not approaches zero. The spectrum of the impurity-induced states is completely different in the topological regime. In this regime the induced superconducting pairing is a p wave, and we find that the energy of the bound states: (i) depends very strongly on u_{imp} , (ii) it is strongly asymmetric with respect to $u_{\text{imp}} = 0$, and (iii) it can go to zero for finite (negative) values of u_{imp} [37]. This can be seen in Fig. 2(a) where the dependence of ω^* on $u_{\text{imp}}\rho_{F,\text{N}}$ [$\rho_{F,\text{N}}$ being the DOS of the semiconductor (N) at its Fermi energy $E_{F,\text{N}}$] for different values of the Zeeman splitting $V_x > V_x^c$.

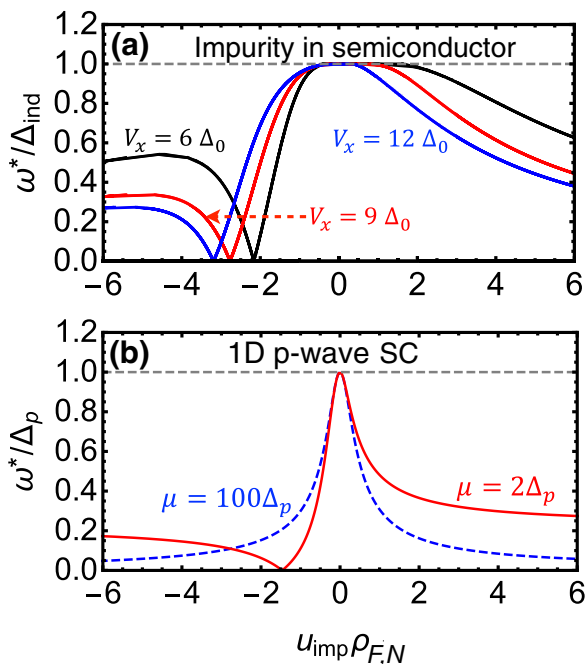


FIG. 2. (a) Spectrum of impurity-induced bound states for the 1D N/SC heterostructure as a function of $u_{\text{imp}}\rho_{F,N}$ for the case (a) of Fig. 1 and $V_x > V_x^c$. Here $k_{F,N}^2/(2m_N) = 1.5\Delta_0$, $\alpha_{SO}k_{F,N} = 4.2\Delta_0$, $\Gamma_t = 5\Delta_0$, $V_x \approx 5.2\Delta_0$. (b) Spectrum of impurity-induced bound states for a 1D p -wave SC as a function of $u_{\text{imp}}\rho_{F,N}$ for different values of μ .

The results shown in Fig. 2(a) can be qualitatively understood considering a scalar impurity Eq. (4) in a 1D p -wave superconductor for which:

$$H_{\text{pSC}} = \sum_{k_x, \sigma, \sigma'} [c_{k_x, \sigma}^\dagger (k_x^2/2m - \mu)\sigma_0 c_{k_x, \sigma'} + i\Delta_p(k_x/k_F) c_{k_x, \sigma}^\dagger \mathbf{d}_{k_x} \cdot \boldsymbol{\sigma} \sigma_y c_{-k_x, \sigma'}^\dagger + \text{H.c.}],$$

where $\Delta_p(k_x/k_F) = -\Delta_p(-k_x/k_F)$ is the amplitude of the superconducting p -wave pairing and \mathbf{d}_{k_x} is the unit vector characterizing the polarization of the triplet state [54]. In this case $T(\omega) = u_{\text{imp}}[\tau_z - u_{\text{imp}} \int dk_x G_{\text{p-SC}}(\omega, k_x)]^{-1}$, where $G_{\text{p-SC}}(\omega, k_x) = (\omega + i\eta - H_{\text{p-SC}})^{-1}$. Due to the 1D nature of the carriers, one finds that, at low energies, the density of states is strongly dependent on their energy ϵ : $\rho(\epsilon) \approx 1/\sqrt{\epsilon}$. This fact makes the energy of the impurity bound state strongly dependent on u_{imp} when μ_N is close to the bottom of the band. This is shown in Fig. 2(b) where we can see that the energy of the bound state depends strongly on u_{imp} when μ is small (the solid line) and fairly weakly for large μ (the dashed line) [55]. We should emphasize that this asymmetry effect is very relevant for 1D topological SC wires supporting MZMs in which typically μ_N must be quite small, i.e., $|\mu_N| < \sqrt{V_x^2 - \Delta_{\text{ind}}^2}$ [46–49].

In the most recent realizations of 1D topological SC wires [9,19–21] the SM and the interface between the SM and the SC are of very high quality so that very few impurities are expected to be present in the SM or at the interface. On the other hand, the SC (i.e., aluminum) is disordered. Therefore, henceforth we consider the situation in which the impurities are located in the SC. In this case, using Eq. (9)

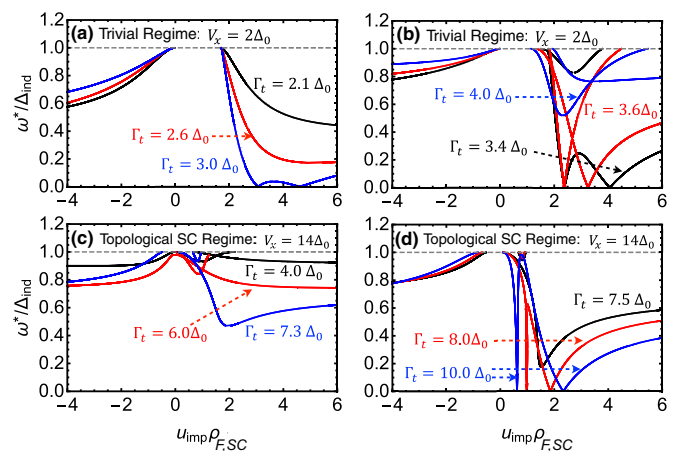


FIG. 3. Spectrum of impurity-induced bound states as function of $u_{\text{imp}}\rho_{F,SC}$ for the 1D N/SC heterostructure when the impurity is located in the SC in (a) and (b) the trivial regime and (c) and (d) the topological regime. Here $k_{F,N}^2/(2m_N) = 1.5\Delta_0$, $\mu_N = 1.5\Delta_0$, $\alpha_{SO}k_{F,N} = 4.2\Delta_0$, $k_{F,N}/k_{F,SC} = 0.3$.

one finds

$$T_{\text{SC}} = \frac{u_{\text{imp}}}{\tau_z \sigma_0 - u_{\text{imp}} \Sigma_{\text{SC,imp}}^{(0)}(\omega) - u_{\text{imp}} \Sigma_{\text{SC,imp}}^{(1)}(\omega)}. \quad (12)$$

For the case in which the SC is an s wave and the tunneling is such that $\hat{h}_T = t\delta(\mathbf{q}_{\parallel})\sigma_z\tau_0$ we obtain

$$\Sigma_{\text{SC,imp}}^{(0)}(\omega) = -\frac{\rho_{F,SC}}{\sqrt{\Delta_0^2 - \omega^2}} [\omega\sigma_0\tau_0 + \Delta_0\sigma_y\tau_y] \quad (13)$$

$$\Sigma_{\text{SC,imp}}^{(1)}(\omega) = \int d\mathbf{k}_{\parallel} \int d\mathbf{k}_{\perp} G_{\text{SC}}^{(0)}(\mathbf{k}_{\parallel}, \mathbf{k}_{\perp}, \omega) \times \Sigma_{\text{SC},t}(\mathbf{k}_{\parallel}, \omega) G_{\text{SC}}(\mathbf{k}_{\parallel}, \mathbf{k}_{\perp}, \omega), \quad (14)$$

with $\Sigma_{\text{SC},t}(\mathbf{k}_{\parallel}, \omega)$ given by Eq. (7). One can show that the strength of the second term $\Sigma_{\text{SC,imp}}^{(1)}(\omega)$ is proportional to the dimensionless parameter $\alpha_{sWS} = \frac{\Gamma_t}{E_{F,N}} \frac{k_{F,N}}{k_{F,SC}}$ (see the Supplemental Material [50] Sec. I for details) where $k_{F,N}$, $k_{F,SC}$ are the Fermi momenta in the N and SC, respectively.

Figure 3(a) shows the spectrum of the impurity-induced states as a function of $u_{\text{imp}}\rho_{F,SC}$ for the 1D case in which the N/SC heterostructure is in the topologically trivial phase $V_x = 2\Delta_0 < V_x^{(c)}$ and different values of Γ_t . In the limit $\alpha_{sWS} \rightarrow 0$, $t \neq 0$ (i.e., $\Sigma_{\text{SC,imp}}^{(1)} \rightarrow 0$ and $\Delta_{\text{ind}} \neq 0$), we find bound states close to the gap edge. As α_{sWS} increases, the interplay between $\Sigma_{\text{SC,imp}}^{(0)}$ and $\Sigma_{\text{SC,imp}}^{(1)}$ may lead to low-lying subgap states as shown in Figs. 3(a) and 3(b). The results of Fig. 3(b) also show that as Γ_t increases the spectrum of the impurity-induced bound states becomes more asymmetric with respect to $u_{\text{imp}} = 0$ as we have found for the case in which the impurity is located in the N. It is very interesting to notice that, contrary to the case when an impurity is located in the N, see Fig. 2(a) in the Supplemental Material [50], an impurity in the SC may lead to low-lying subgap states with $\omega^* \rightarrow 0$ in the trivial regime. Figures 3(c) and 3(d) show the results when the N/SC heterostructure is in the topological phase $V_x = 14\Delta_0 > V_x^{(c)}$. One can see that the spectrum is strongly asymmetric in this case even for relatively small values of Γ_t ,

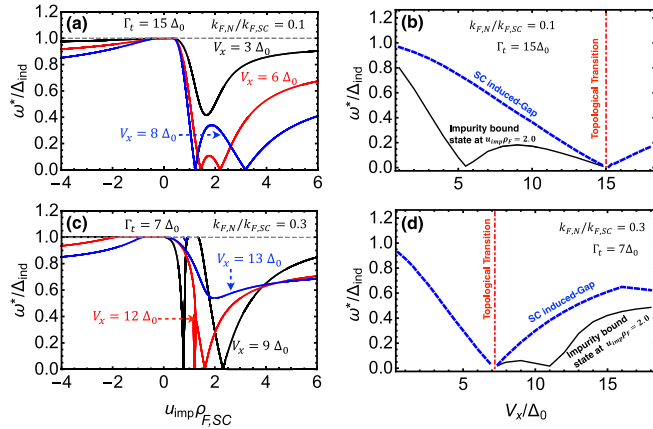


FIG. 4. Effect of V_x on the impurity-induced bound states spectrum. (a) and (b) $\Gamma_t = 15\Delta_0$, $k_{F,N}/k_{F,SC} = 0.1$. In (a) $V_x < V_x^{(c)}$. (c) and (d) $\Gamma_t = 7\Delta_0$, $k_{F,N}/k_{F,SC} = 0.3$. In (c) $V_x > V_x^{(c)}$. (b) and (d) show the evolution of impurity-induced bound states (the black solid line) for fixed $u_{\text{imp}}\rho_F = 2.0$.

Fig. 3(c). For larger Γ_t we find that also in the topological phase the impurity can induce zero-energy bound states for relatively small values of $u_{\text{imp}}\rho_{F,SC}$, Fig. 3(d). These results suggest that in the topological phase the value of u_{imp} necessary to induce a zero-energy bound state decreases as Γ_t increases. Thus, there is an optimal value of Γ_t for which the induced gap is large and, at the same time, impurities in the SC do not result in significant subgap density of states. The effect of V_x on the spectrum of the impurity-induced bound states is summarized by the results shown in Fig. 4. Figures 4(a) and 4(c) show how, for fixed Γ_t , V_x affects the dependence of the spectrum on u_{imp} for the case when $V_x < V_x^{(c)}$ (a), and $V_x > V_x^{(c)}$ (c). As one can see there is a threshold value of V_x for the emergence of bound states with $\omega^* \rightarrow 0$ both in the trivial and in the topological regimes. Figures 4(b) and 4(d) show the evolution of ω^* with V_x for fixed u_{imp} for the same values of Γ_t and $k_{F,N}/k_{F,SC}$ used in (a) and (c), respectively. From the results of Fig. 4 we see that zero-energy impurity-induced bound states may appear in both the topological and the trivial regimes by tuning the magnetic field.

Considering that V_x and Γ_t are two of the key parameters that can be controlled in experiments to realize MZMs in proximitized nanowires, the knowledge of where on the (V_x, Γ_t) plane $\omega^* = 0$ is of great importance for the realization of topological qubits based on such systems [56–59]. Figures 5(a) and 5(b) show in gray-blue (yellow) the regions on the (V_x, Γ_t) plane for which there exist a finite value of u_{imp} such that $\omega^* = 0$ ($\omega^* < 0.6\Delta_{\text{ind}}$). The red dashed line shows the boundary between trivial and topological regimes. The horizontal dashed line in Fig. 5(a) [Fig. 5(b)] identifies the values of Γ_t for which the results of Figs. 4(a) and 4(b) [Figs. 4(c) and 4(d)] were obtained. As follows from Fig. 5(a), the area where $\omega^* = 0$ is rather large in the trivial regime and becomes smaller in the topological one when $k_{F,N}/k_{F,SC} \ll 1$. As the ratio $k_{F,N}/k_{F,SC}$ increases the area where $\omega^* = 0$ decreases in the trivial phase and increases in the topological phase as shown by Fig. 5(b). Thus, the ratio of $k_{F,N}/k_{F,SC}$ is an important parameter when trying to reduce disorder effects in

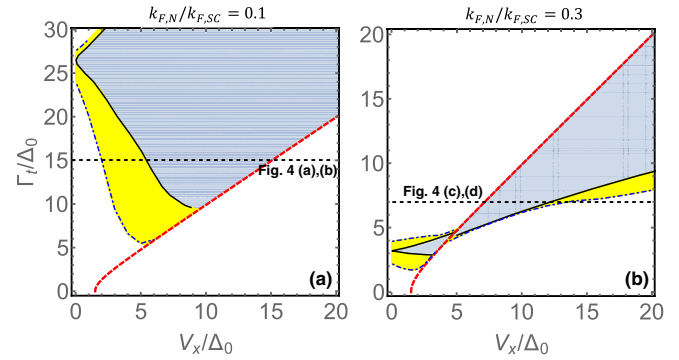


FIG. 5. Phase diagram on the (V_x, Γ_t) plane identifying the regions, shown in gray (yellow) for which $\omega^* = 0$ ($\omega^* < 0.6\Delta_{\text{ind}}$) for some finite value of u_{imp} (not for the fixed value of u_{imp}). The red dashed line shows the boundary between trivial and topological regimes. The horizontal dashed line is placed at the value of Γ_t for which the results of Fig. 4 were obtained. (An evolution of bound states for fixed u_{imp} is shown in the Supplemental Material [50] Sec. IV.) Here $k_{F,N}^2/(2m_N) = 1.5\Delta_0$, $\alpha_{\text{SO}}k_{F,N} = 4.2\Delta_0$.

superconducting heterostructures. For aluminum-based proximitized nanowires this parameter is quite small $k_{F,N}/k_{F,SC} \ll 1$. The parameter α_{SO} can be controlled experimentally by changing the back-gate voltage in proximitized nanowires [60,61] so the propensity for the formation of impurity-induced bound states we predict, see Fig. 5, can be tested experimentally.

Conclusions. We have studied impurity-induced subgap states in superconductor-based heterostructures. In the case of proximitized nanowires we find that in these structures there is a large region in parameter space for which the impurities in the superconductor can induce low-energy states even when the superconductor is purely an s wave. Our Rapid Communication presents results for the spectrum of the bound states induced by a single impurity and so is complementary to the previous studies that considered the case of many weak impurities [31–36,38,42,44,62] via disorder-averaging techniques. Our results are directly relevant to experimental situations in which the impurity density is low and disorder averaging is not justified. In addition, they are instrumental to extend the study of the effect of many impurities via disorder averaging to the unitary limit, i.e., the limit of strong impurities, both for the case when the impurities are located in the SM and for the case when they are located in the superconductor.

Our results provide guidance for the optimization of superconductor-semiconductor heterostructures: Although a strong tunneling is beneficial to obtain a large gap, it also enhances the effect of the impurities located in the s -wave superconductor on the superconducting state induced in the semiconductor. Therefore, we find that, when the effect of impurities is included, the optimal coupling to the superconductor is not strong but intermediate, i.e., $\Gamma_t \sim \Delta_0$.

Acknowledgments. E.R. acknowledges support from NSF CAREER Grants No. DMR-1455233, No. ARO-W911NF-16-1-0387, and No. ONR-N00014-16-1-3158.

- [1] M. Z. Hasan and C. L. Kane, *Rev. Mod. Phys.* **82**, 3045 (2010).
- [2] C. W. J. Beenakker, *Annu. Rev. Condens. Matter Phys.* **4**, 113 (2013).
- [3] J. Alicea, *Rep. Prog. Phys.* **75**, 076501 (2012).
- [4] M. Leijnse and K. Flensberg, *Semicond. Sci. Technol.* **27**, 124003 (2012).
- [5] T. D. Stanescu and S. Tewari, *J. Phys.: Condens. Matter* **25**, 233201 (2013).
- [6] S. R. Elliott and M. Franz, *Rev. Mod. Phys.* **87**, 137 (2015).
- [7] S. D. Sarma, M. Freedman, and C. Nayak, *npj Quantum Information* **1**, 15001 (2015).
- [8] M. Sato and S. Fujimoto, *J. Phys. Soc. Jpn.* **85**, 072001 (2016).
- [9] R. M. Lutchyn, E. P. A. M. Bakkers, L. P. Kouwenhoven, P. Krogstrup, C. M. Marcus, and Y. Oreg, [arXiv:1707.04899](https://arxiv.org/abs/1707.04899).
- [10] V. Mourik, K. Zuo, S. M. Frolov, S. R. Plissard, E. P. A. M. Bakkers, and L. P. Kouwenhoven, *Science* **336**, 1003 (2012).
- [11] L. P. Rokhinson, X. Liu, and J. K. Furdyna, *Nat. Phys.* **8**, 795 (2012).
- [12] M. T. Deng, C. L. Yu, G. Y. Huang, M. Larsson, P. Caroff, and H. Q. Xu, *Nano Lett.* **12**, 6414 (2012).
- [13] H. O. H. Churchill, V. Fatemi, K. Grove-Rasmussen, M. T. Deng, P. Caroff, H. Q. Xu, and C. M. Marcus, *Phys. Rev. B* **87**, 241401(R) (2013).
- [14] A. Das, Y. Ronen, Y. Most, Y. Oreg, M. Heiblum, and H. Shtrikman, *Nat. Phys.* **8**, 887 (2012).
- [15] A. D. K. Finck, D. J. Van Harlingen, P. K. Mohseni, K. Jung, and X. Li, *Phys. Rev. Lett.* **110**, 126406 (2013).
- [16] S. Nadj-Perge, I. K. Drozdov, J. Li, H. Chen, S. Jeon, J. Seo, A. H. MacDonald, B. A. Bernevig, and A. Yazdani, *Science* **346**, 602 (2014).
- [17] M. T. Deng, C. L. Yu, G. Y. Huang, M. Larsson, P. Caroff, and H. Q. Xu, *Sci. Rep.* **4**, 7261 (2014).
- [18] A. P. Higginbotham, S. M. Albrecht, G. Kiršanskas, W. Chang, F. Kuemmeth, P. Krogstrup, T. S. Jespersen, J. Nygård, K. Flensberg, and C. M. Marcus, *Nat. Phys.* **11**, 1017 (2015).
- [19] S. M. Albrecht, A. P. Higginbotham, M. Madsen, F. Kuemmeth, T. S. Jespersen, J. Nygård, P. Krogstrup, and C. M. Marcus, *Nature (London)* **531**, 206 (2016).
- [20] M. T. Deng, S. Vaitiekėnas, E. B. Hansen, J. Danon, M. Leijnse, K. Flensberg, J. Nygård, P. Krogstrup, and C. M. Marcus, *Science* **354**, 1557 (2016).
- [21] H. Zhang *et al.*, Ballistic Majorana nanowire devices, [arXiv:1603.04069](https://arxiv.org/abs/1603.04069) (2016).
- [22] H. Zhang, Ö. Gül, S. Conesa-Boj, M. P. Nowak, M. Wimmer, K. Zuo, V. Mourik, F. K. de Vries, J. van Veen, M. W. A. de Moor, J. D. S. Bommer, D. J. van Woerkom, D. Car, S. R. Plissard, E. P. A. M. Bakkers, M. Quintero-Pérez, M. C. Cassidy, S. Koelling, S. Goswami, K. Watanabe, T. Taniguchi, and L. P. Kouwenhoven, *Nat. Commun.* **8**, 16025 (2017).
- [23] Ö. Gül, H. Zhang, J. D. S. Bommer, M. W. A. de Moor, D. Car, S. R. Plissard, E. P. A. M. Bakkers, A. Geresdi, K. Watanabe, T. Taniguchi, and L. P. Kouwenhoven, *Nat. Nanotechnol.* **13**, 192 (2018).
- [24] H. Zhang, C.-X. Liu, S. Gazibegovic, D. Xu, J. A. Logan, G. Wang, N. van Loo, J. D. S. Bommer, M. W. A. de Moor, D. Car, R. L. M. Op het Veld, P. J. van Veldhoven, S. Koelling, M. A. Verheijen, M. Pendharkar, D. J. Pennachio, B. Shojaei, J. S. Lee, C. J. Palmstrøm, E. P. A. M. Bakkers, S. D. Sarma, and L. P. Kouwenhoven, *Nature (London)* **556**, 74 (2018).
- [25] A. V. Balatsky, I. Vekhter, and J.-X. Zhu, *Rev. Mod. Phys.* **78**, 373 (2006).
- [26] O. Motrunich, K. Damle, and D. A. Huse, *Phys. Rev. B* **63**, 224204 (2001).
- [27] P. W. Brouwer, M. Duckheim, A. Romito, and F. von Oppen, *Phys. Rev. Lett.* **107**, 196804 (2011).
- [28] P. W. Brouwer, M. Duckheim, A. Romito, and F. von Oppen, *Phys. Rev. B* **84**, 144526 (2011).
- [29] T. D. Stanescu, R. M. Lutchyn, and S. D. Sarma, *Phys. Rev. B* **84**, 144522 (2011).
- [30] A. R. Akhmerov, J. P. Dahlhaus, F. Hassler, M. Wimmer, and C. W. J. Beenakker, *Phys. Rev. Lett.* **106**, 057001 (2011).
- [31] A. C. Potter and P. A. Lee, *Phys. Rev. B* **83**, 184520 (2011).
- [32] A. C. Potter and P. A. Lee, *Phys. Rev. B* **84**, 059906(E) (2011).
- [33] A. M. Lobos, R. M. Lutchyn, and S. D. Sarma, *Phys. Rev. Lett.* **109**, 146403 (2012).
- [34] R. M. Lutchyn, T. D. Stanescu, and S. D. Sarma, *Phys. Rev. B* **85**, 140513(R) (2012).
- [35] J. D. Sau, S. Tewari, and S. D. Sarma, *Phys. Rev. B* **85**, 064512 (2012).
- [36] G. Tkachov, *Phys. Rev. B* **87**, 245422 (2013).
- [37] J. D. Sau and E. Demler, *Phys. Rev. B* **88**, 205402 (2013).
- [38] J. D. Sau and S. D. Sarma, *Phys. Rev. B* **88**, 064506 (2013).
- [39] S. Takei, B. M. Fregoso, H.-Y. Hui, A. M. Lobos, and S. D. Sarma, *Phys. Rev. Lett.* **110**, 186803 (2013).
- [40] W. DeGottardi, D. Sen, and S. Vishveshwara, *Phys. Rev. Lett.* **110**, 146404 (2013).
- [41] I. Adagideli, M. Wimmer, and A. Teker, *Phys. Rev. B* **89**, 144506 (2014).
- [42] H.-Y. Hui, J. D. Sau, and S. D. Sarma, *Phys. Rev. B* **92**, 174512 (2015).
- [43] S. S. Hegde and S. Vishveshwara, *Phys. Rev. B* **94**, 115166 (2016).
- [44] W. S. Cole, J. D. Sau, and S. D. Sarma, *Phys. Rev. B* **94**, 140505 (2016).
- [45] P. W. Anderson, *J. Phys. Chem. Solids* **11**, 26 (1959).
- [46] J. D. Sau, R. M. Lutchyn, S. Tewari, and S. D. Sarma, *Phys. Rev. Lett.* **104**, 040502 (2010).
- [47] J. Alicea, *Phys. Rev. B* **81**, 125318 (2010).
- [48] R. M. Lutchyn, J. D. Sau, and S. D. Sarma, *Phys. Rev. Lett.* **105**, 077001 (2010).
- [49] Y. Oreg, G. Refael, and F. von Oppen, *Phys. Rev. Lett.* **105**, 177002 (2010).
- [50] See Supplemental Material at <http://link.aps.org/supplemental/10.1103/PhysRevB.97.161408> for (I) details on the derivation of the T-matrix expression for the case when the impurity is located in the superconductor, see Eqs. (13)–(15) of the main text; (II) the relation between the parameters values used in our calculations and the parameters values of current experiments on quasi 1D semiconductor- superconductor (N-SC) heterostructures; (III) additional results for the case when the impurity is located in the semiconductor, (IV) dependence on Zeeman splitting for the impurity strength necessary to induce a zero energy bound state.
- [51] L. P. Gor'kov and E. I. Rashba, *Phys. Rev. Lett.* **87**, 037004 (2001).
- [52] P. A. Frigeri, D. F. Agterberg, A. Koga, and M. Sigrist, *Phys. Rev. Lett.* **92**, 097001 (2004).
- [53] C. Triola, D. M. Badiane, A. V. Balatsky, and E. Rossi, *Phys. Rev. Lett.* **116**, 257001 (2016).
- [54] A. P. Mackenzie and Y. Maeno, *Rev. Mod. Phys.* **75**, 657 (2003).

- [55] A similar asymmetry for the energy of bound states with respect to $u_{\text{imp}} = 0$ has also been found for the case of d -wave superconductors [63]: Also in that case such asymmetry is due to the dependence of the DOS on the energy.
- [56] T. Hyart, B. van Heck, I. C. Fulga, M. Burrello, A. R. Akhmerov, and C. W. J. Beenakker, *Phys. Rev. B* **88**, 035121 (2013).
- [57] D. Aasen, M. Hell, R. V. Mishmash, A. Higginbotham, J. Danon, M. Leijnse, T. S. Jespersen, J. A. Folk, C. M. Marcus, K. Flensberg, and J. Alicea, *Phys. Rev. X* **6**, 031016 (2016).
- [58] S. Plugge, A. Rasmussen, R. Egger, and K. Flensberg, *New J. Phys.* **19**, 012001 (2017).
- [59] T. Karzig, C. Knapp, R. Lutchyn, P. Bonderson, M. Hastings, C. Nayak, J. Alicea, K. Flensberg, S. Plugge, Y. Oreg, C. Marcus, and M. H. Freedman, *Phys. Rev. B* **95**, 235305 (2017).
- [60] S. Vaitiekėnas, M. T. Deng, J. Nygård, P. Krogstrup, and C. M. Marcus, [arXiv:1710.04300](https://arxiv.org/abs/1710.04300).
- [61] A. E. Antipov, A. Bargerbos, G. W. Winkler, B. Bauer, E. Rossi, and R. M. Lutchyn, [arXiv:1801.02616](https://arxiv.org/abs/1801.02616).
- [62] C.-X. Liu, J. D. Sau, T. D. Stanescu, and S. D. Sarma, *Phys. Rev. B* **96**, 075161 (2017).
- [63] W. A. Atkinson, P. J. Hirschfeld, A. H. MacDonald, and K. Ziegler, *Phys. Rev. Lett.* **85**, 3926 (2000).

Supplementary Information for Impurity-induced states in superconducting heterostructures”

Dong E. Liu,¹ Enrico Rossi,² and Roman M. Lutchyn¹

¹Station Q, Microsoft Research, Santa Barbara, California 93106-6105, USA

²Department of Physics, College of William and Mary, Williamsburg, VA 23187, USA

(Dated: March 31, 2018)

In this supplementary material we provide: (I) details on the derivation of the T-matrix expression for the case when the impurity is located in the superconductor, see Eq. (13-15) of the main text; (II) the relation between the parameters values used in our calculations and the parameters values of current experiments on quasi 1D semiconductor-superconductor (N-SC) heterostructures; (III) additional results for the case when the impurity is located in the semiconductor, (IV) dependence on V_x of the impurity strength necessary to induce a zero energy $\omega^* = 0$ impurity-induced bound state.

I. T-MATRIX CALCULATION FOR AN IMPURITY IN THE SUPERCONDUCTOR

The scattering T-matrix for a single impurity in a superconductor proximity-coupled to a semiconductor nanowire can be described by a diagrammatic representation shown in Fig. 1:

$$\begin{aligned}
 T_{SC}(\omega) &= u_{imp}\tau_z\sigma_0 + u_{imp}^2\tau_z\sigma_0 \cdot \left(\Sigma_{SC,imp}^{(0)}(\omega) + \Sigma_{SC,imp}^{(1)}(\omega) \right) \cdot \tau_z\sigma_0 \\
 &\quad + u_{imp}^3\tau_z\sigma_0 \cdot \left(\Sigma_{SC,imp}^{(0)}(\omega) + \Sigma_{SC,imp}^{(1)}(\omega) \right) \cdot \tau_z\sigma_0 \cdot \left(\Sigma_{SC,imp}^{(0)}(\omega) + \Sigma_{SC,imp}^{(1)}(\omega) \right) \cdot \tau_z\sigma_0 + \dots \\
 &= \frac{u_{imp}}{\tau_z\sigma_0 - u_{imp}\Sigma_{SC,imp}^{(0)}(\omega) - u_{imp}\Sigma_{SC,imp}^{(1)}(\omega)}, \tag{1}
 \end{aligned}$$

where $\Sigma_{SC,imp}^{(0)}(\omega)$ represents the contribution to the self-energy for a clean s-wave superconductor:

$$\Sigma_{SC,imp}^{(0)}(\omega) = \sum_{\vec{k}} G_{SC}^{(0)}(\omega, \vec{k}) = \rho_{F,SC} g^{qc}(\omega) = -\frac{\rho_{F,SC}}{\sqrt{\Delta_0^2 - \omega^2}} \begin{pmatrix} \omega\sigma_0 & (\Delta_0 i\sigma_y)^\dagger \\ (\Delta_0 i\sigma_y) & \omega\sigma_0 \end{pmatrix}. \tag{2}$$

The expression above corresponds to Eq. (13) of the main text. The second term $\Sigma_{SC,imp}^{(1)}(\omega)$ represents a process in which an electron tunnels between the SC and the semiconductor, and scatters off the impurity

$$\Sigma_{SC,imp}^{(1)}(\omega) = \int d\mathbf{k}_{\parallel} d\mathbf{k}_{1,\perp} d\mathbf{k}_{2,\perp} G_{SC}^{(0)}(\mathbf{k}_{\parallel}, \mathbf{k}_{1,\perp}, \omega) \Sigma_{SC,t}(\mathbf{k}_{\parallel}, \omega) G_{SC}(\mathbf{k}_{\parallel}, \mathbf{k}_{2,\perp}, \omega) \tag{3}$$

$$= t^2 \int d\mathbf{k}_{\parallel} d\mathbf{k}_{1,\perp} d\mathbf{k}_{2,\perp} G_{SC}^{(0)}(\mathbf{k}_{\parallel}, \mathbf{k}_{1,\perp}, \omega) \cdot \tau_z\sigma_0 \cdot G_N(\mathbf{k}_{\parallel}, \omega) \cdot \tau_z\sigma_0 \cdot G_{SC}^{(0)}(\mathbf{k}_{\parallel}, \mathbf{k}_{2,\perp}, \omega). \tag{4}$$

$$\begin{aligned}
 T_{SC}(\omega) &= \begin{array}{c} \times \quad \times \\ | \quad | \\ \hline \rho_F \Sigma_{SC,imp}^{(0)}(\omega) \quad \rho_F \Sigma_{SC,imp}^{(1)}(\omega) \end{array} \\
 &\quad + \dots
 \end{aligned}$$

FIG. 1: Diagrammatic representation of the T-matrix for a single impurity placed in the superconductor of a SC/SM heterostructure. Processes that involve two scatterings can be of two types: 1) processes in which the electrons do not leave the SC between the two scatterings, 2) processes in which the electrons travel through the N in between the two scatterings. The meaning of the different lines is the following: double solid line (red), propagator in s-wave SC; dashed-solid line (black), propagator in semiconductor wire with proximity induced superconducting gap; cross head - dashed line, scattering off the impurity.

Here t is tunneling matrix element between the SC and nanowire (N), G_N is the dressed semiconductor Green function (in proximity to a clean SC). We assume that the momentum parallel to the SC-N interface is conserved.

The largest contribution to the scattering in the SC comes from on-shell processes (i.e. close to the Fermi surface). Therefore, it's convenient to introduce $\delta\mathbf{k} \equiv (\delta k, \hat{\Omega})$, where $\delta k = |\mathbf{k} - \mathbf{k}_{F,SC}| \ll k_{F,SC}$ and $\hat{\Omega} \equiv \mathbf{k}/|\mathbf{k}|$. With this notation we obtain:

$$\Sigma_{SC,imp}^{(1)}(\omega) = \frac{L_z k_{F,N}}{E_{F,N}} t^2 \int d\hat{\Omega} \left(\frac{1}{k_{F,SC} L_z} \int d\delta k G_{SC}^{(0)}(\omega; \delta k, \hat{\Omega}) \right) \cdot \tau_z \sigma_0 \cdot R(\omega) \cdot \tau_z \sigma_0 \cdot \int d\hat{\Omega} \left(\frac{1}{k_{F,SC} L_z} \int d\delta k G_{SC}^{(0)}(\omega; \delta k, \hat{\Omega}) \right), \quad (5)$$

where $k_{F,N}$ and $E_{F,N}$ are the Fermi wavevector and Fermi energy in the semiconductor wire, respectively, $\rho_{F,SC}$ is the normal-state density of states (DOS), at the Fermi energy, of the SC, and

$$R(\omega) \equiv E_{F,N} \int \frac{d\tilde{\mathbf{k}}_{\parallel}}{2\pi} G_N(\omega; \tilde{\mathbf{k}}_{\parallel}); \quad \text{with } \tilde{\mathbf{k}}_{\parallel} = \frac{\mathbf{k}_{\parallel}}{k_{F,N}}. \quad (6)$$

Notice that the DOS contributing to the N-SC tunneling amplitude is given by $\rho_{F,SC}^t = \rho_{F,SC}/(k_{F,SC} L_z)$. Assuming the bare SC Green's function $G_{SC}(\omega; k, \hat{\Omega})$ to be isotropic and, thus, independent of $\hat{\Omega}$, one can simplify the expression for $\Sigma_{SC,imp}^{(1)}(\omega)$:

$$\Sigma_{SC,imp}^{(1)}(\omega) = \alpha_{SwS} \rho_{F,SC} [g^{qc}(\omega) \cdot \tau_z \sigma_0 \cdot R(\omega) \cdot \tau_z \sigma_0 \cdot g^{qc}(\omega)] \quad (7)$$

where

$$\alpha_{SwS} = \frac{\Gamma_t}{E_{F,N}} \frac{k_{F,N}}{k_{F,SC}}; \quad \text{with } \Gamma_t = \pi |t|^2 \rho_{F,SC}^t; \quad (8)$$

$$g^{qc}(\omega) = \frac{1}{\rho_{F,SC}} \sum_{\delta\mathbf{k}} G_{SC}^{(0)}(\delta\mathbf{k}, \omega). \quad (9)$$

Notice that the presence of the vertex matrix $\tau_z \sigma_0$ flips the position of the zero energy solutions from $u_{imp}^* \rho_{F,SC} < 0$ to $u_{imp}^* \rho_{F,SC} > 0$ (please compare Fig. 2 with Fig. 3 and 4 in the main text).

II. RELATION BETWEEN PARAMETERS VALUES USED IN THE CALCULATION AND EXPERIMENTAL VALUES

Here, we briefly explain how to choose the numerical parameters based on relevant experimental systems [1–5]. We consider aluminum/InSb (SC/N), and choose for the superconducting gap of the bulk SC $\Delta_0 = 0.2$ meV, and for the Rashba spin-orbit coupling strength of the semiconductor $\alpha_{SO} = 0.2 - 1$ eV \cdot \AA . We assume the energy dispersion of the semiconductor (without Rashba spin-orbit coupling and Zeeman splitting) to be $\epsilon_{N,k} = \frac{k^2}{2m_{\text{eff}}} - \mu_N = \frac{k_{F,N}^2}{2m_{\text{eff}}} (\hat{k}^2 - 1)$ with $\hat{k} = k/k_{F,N}$. We assume $m_{\text{eff}} = 0.014m_e$ with m_e the electron's mass. Including both Rashba coupling and Zeeman splitting, the energy spectrum becomes: $E_N(\hat{k}) = \frac{k_{F,N}^2}{2m_{\text{eff}}} (\hat{k}^2 - 1) \pm \sqrt{V_x^2 + (\hat{k} k_{F,N} \alpha_{SO})^2}$ with the Fermi surface being identified by the value of k^* such that $E_N(k^*) = 0$. The Rashba spin-orbit energy can then be expressed as $E_{SO} = \hat{k}^* k_{F,N} \alpha_{SO}$. The results of the main text were obtained setting $\alpha_{SO} = 0.8$ eV \cdot \AA and $\frac{k_{F,N}^2}{2m_{\text{eff}}} = 1.5\Delta_0$, corresponding to $k_{F,N} \alpha_{SO} = 4.22\Delta_0$.

III. ADDITIONAL RESULTS FOR CASE WHEN THE IMPURITY IS IN THE SEMICONDUCTOR

In this section, we consider the case in which the impurity is in the semiconductor, and show that low energy bound states appear even in the topological trivial regime, if the chemical potential is large. For this section we assume $\Delta_0 = 0.2$ meV, $m_{\text{eff}} = 0.014m_e$, $\alpha_{SO} = 0.22$ eV \cdot \AA , and $\frac{k_{F,N}^2}{2m_{\text{eff}}} = 10.0\Delta_0$, and therefore $k_{F,N} \alpha_{SO} = 3.0\Delta_0$. Fig. 2 (a) and (b) show how ω^* depends on $u_{imp} \rho_{F,N}$ for different values of the Zeeman splitting V_x . Fig. 2 (a) (Fig. 2 (b)) shows the results for $V_x < V_x^c$ ($V_x > V_x^c$). The dashed lines show the value of Δ_{ind} . Interestingly, we can see that impurity bound states (albeit with non-zero energy) can appear even in the topologically trivial regime. We also notice that

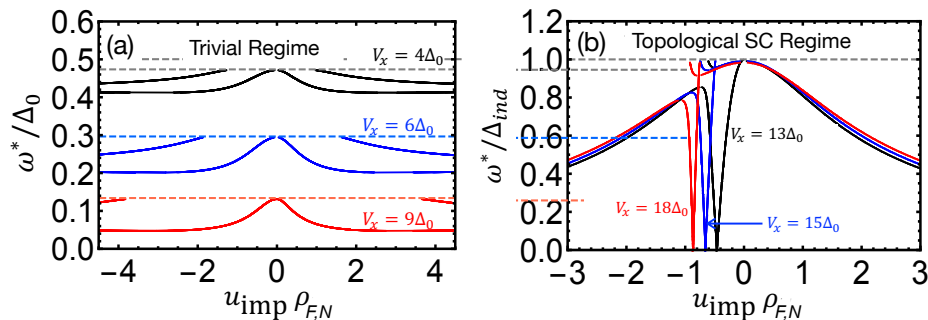


FIG. 2: Spectrum of impurity-induced bound states for 1D N/SC heterostructure as a function of $u_{\text{imp}}\rho_{F,N}$ for the case in which the impurity is in the semiconductor. $k_{F,N}^2/(2m_w) = 10\Delta_0$, $\alpha k_F = 3\Delta_0$, $\Gamma_t = 5\Delta_0$. Trivial regime, (a), and topological regime (b). Here the topological transition occurs at $V_x^c \approx 11.2\Delta_0$

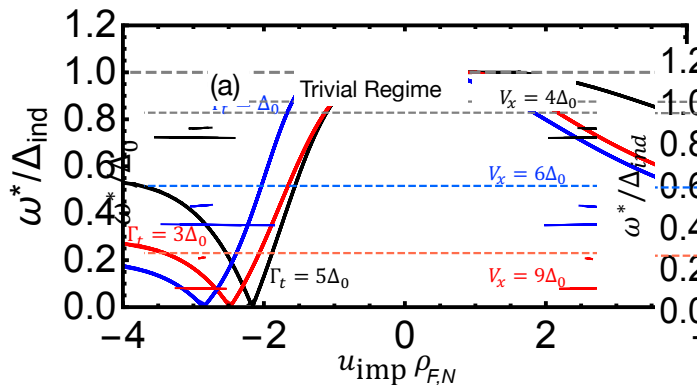


FIG. 3: Spectrum of impurity-induced bound states as a function of $u_{\text{imp}}\rho_{F,N}$ for 1D N/SC heterostructure for the case when the impurity is in the semiconductor for fixed $V_x = 6\Delta_0 > V_x^{(c)}$, and different values of Γ_t . $k_{F,N}^2/(2m_w) = 10\Delta_0$, $\alpha k_F = 3\Delta_0$.

the bound states shift to the induced-gap edge if we decrease the parameter $\frac{k_{F,N}^2}{2m_{\text{eff}}}$. We see that in the trivial regime the energy of the impurity-induced bound states becomes smaller as V_x increases but it never goes to zero. We also notice that the energy of the bound states depends weakly on u_{imp} with a slight asymmetry of the spectrum with respect to the sign of the potential of the impurity.

We now consider how the interface coupling Γ_t affect the spectrum when the impurity is located in the SM. The induced gap is proportional to Γ_t : $\Delta_{\text{ind}} \sim \Gamma_t$. Therefore, as Γ_t increases, the ratio μ/Δ_{ind} becomes smaller causing an increase of the particle-hole asymmetry, in the normal state, close to Fermi level. As a consequence, we that for larger values of Γ_t there will be a stronger asymmetry in the spectrum of impurity bound states (refer to Fig. 2 (a) in the main text), and that a smaller impurity strength $|u_{\text{imp}}|$ will be necessary to induce a zero-energy bound state, as shown in Fig. 3.

IV. DEPENDENCE ON V_x OF THE IMPURITY STRENGTH NECESSARY TO INDUCE A ZERO ENERGY IMPURITY-INDUCED BOUND STATE

Fig. 4 shows how the value of $|u_{\text{imp}}^*\rho_{F,SC}|$ such that $\omega^* = 0$ depends on V_x . For the parameters along the dashed line in Fig. 5 (a) of the main text, Fig. 4 (a) shows that the value of $|u_{\text{imp}}^*\rho_{F,SC}|$ that gives one of the $\omega^* = 0$ solutions decreases and approaches a constant at the topological transition whereas for the other $\omega^* = 0$ solution $|u_{\text{imp}}^*\rho_{F,SC}|$ increases to infinity. For the case shown in Fig. 5 (b) of the main text, Fig. 4 (b) shows that as V_x increases the two zero-energy solutions merge and then disappear.

[1] C. W. J. Beenakker, Annu. Rev. Condens. Matter Phys. **4**, 113 (2013), arXiv:1112.1950.
 [2] J. Alicea, Reports on Progress in Physics **75**, 076501 (2012), 1202.1293.

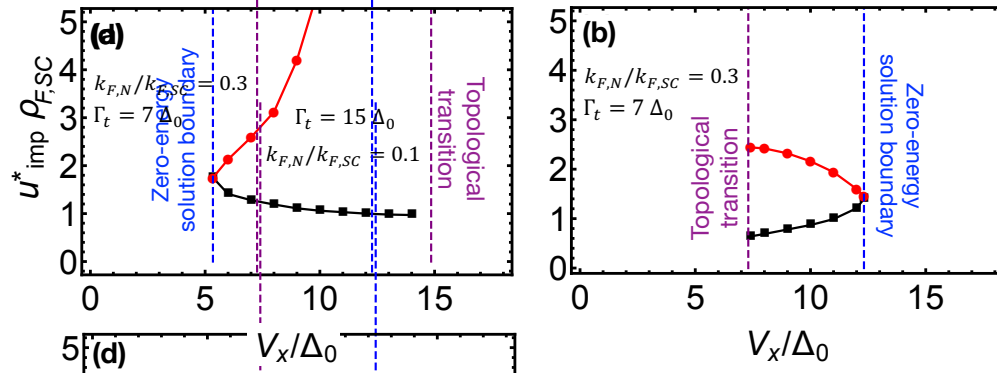


FIG. 4: Impurity strength $|u_{\text{imp}}^* \rho_{F,SC}|$ such that $\omega^* = 0$ as a function of V_x . The parameters chosen are the same as the dashed line in Fig. 4 and 5 of the main text.

- [3] M. Leijnse and K. Flensberg, *Semiconductor Science Technology* **27**, 124003 (2012), 1206.1736.
- [4] T. D. Stanescu and S. Tewari, *Journal of Physics Condensed Matter* **25**, 233201 (2013), 1302.5433.
- [5] R. M. Lutchyn, E. P. A. M. Bakkers, L. P. Kouwenhoven, P. Krogstrup, C. M. Marcus, and Y. Oreg, *ArXiv e-prints* (2017), 1707.04899.